Accepted for publication in Journal of Reinforced Plastics and Composites
Published in December, 2015
DOI: 10.1177/0731684415614087

Mechanical and abrasion wear properties of hydrogenated nitrile butadiene rubber of identical hardness filled with carbon black and silica

E. Padenko[1], P. Berki[2], B. Wetzel[1] and J. Karger-Kocsis[2,3*]

1- Institut für Verbundwerkstoffe GmbH (Institute for Composite Materials), Kaiserslautern University of Technology, D-67663 Kaiserslautern, Germany
2- Department of Polymer Engineering, Budapest University of Technology and Economics, Muegyetem rkp. 3, H-1111 Budapest, Hungary
3- MTA–BME Research Group for Composite Science and Technology, Muegyetem rkp. 3., H-1111 Budapest, Hungary

* author to whom correspondence should be addressed (E-mail:karger@pt.bme.hu)
Submitted to JRPC, Sept. 2015

Abstract

The mechanical and abrasive wear properties of a hydrogenated nitrile rubber (HNBR) filled with 35 part per hundred rubber (phr) carbon black (CB) or silica with and without silane surface treatment (SI-si and SI, respectively), were investigated. Specimens were subjected to dynamic mechanical thermal analysis (DMTA – also to study the Payne effect), mechanical (hardness, tensile modulus, ultimate tensile strength and strain, Mullins effect and tear strength), and fracture mechanical (J-integral) tests. The abrasive coefficient of friction (COF) and wear (specific wear rate, W_s) of the HNBRs of identical hardness were measured against abrasive papers of different grit sizes (P600-P5000).The worn surface of the HNBR systems was inspected in scanning electron microscopy (SEM) and the typical wear mechanisms deduced and discussed. COF did not change with the grit size by contrast to W_s which was markedly reduced with decreasing surface roughness of the abrasive

paper. W_s of the compounds did not vary when wearing against P3000 and P5000 abrasive papers, representing mean surface values of 7 and 5 μm, respectively. This was attributed to a change from abrasion to sliding type wear. HNBR-CB outperformed the silica filled versions with respect to W_s though exhibited the highest COF. No definite correlation could be found between the abrasive wear and the studied DMTA and (fracture) mechanical properties.
Keywords: rubber; filler; abrasive fiction and wear; mechanical properties; J-integral; silane treatment

Introduction

Friction and wear properties of polymers are key parameters for many tribological applications. The wear of polymers is a complex phenomenon that can be classified differently, such as according to the type of the polymers, interaction scale between the wearing counterparts and origin of the wear process (e.g. abrasive. sliding, fretting...) [1]. Rubbers are usually tested under abrasive and sliding conditions. This preference is due to the traditional applications fields of rubbers. For tyres, track pads, rubber coating of pumps and mills for example abrasive, whereas for seals and bushing sliding wear characteristics are critical issues.

Hydrogenated acrylonitrile butadiene rubber (HNBR) exhibits excellent mechanical properties combined with superior heat- and oil resistance [2]. As a consequence, HNBR is widely used in mechanical and automotive engineering. Metal parts, subjected to dry or wet abrasive media are usually covered by rubbers, which necessitates the testing of non-tyre rubber compounds under abrasive conditions, as well. Reports on the sliding and rolling friction and wear of various HNBR-based compounds are already available [3-6]. By contrast, little information is available on the abrasive performance of HNBR gums [7-8].

Albeit wear is considered as a system instead of a material property, efforts have always been in progress to find correlations between wear and mechanical properties. It is well documented in the literature that the hardness of rubbers is inversely proportional with the specific wear rate ([9] and references therein). Therefore, different rubbers of identical hardness should be tested first in order to find possible correlations between the mechanical and wear properties. Following this strategy, the abrasive wear performance oh HNBR compounds containing various

fillers but showing the same hardness was the topic of this study. The fillers selected were carbon black (CB) and silica (SI) with (SI-si) and without additional silanization that occurred during compounding. To guarantee the same hardness of the resulting gums the above nanoscale fillers had similar specific surface areas. To get deeper understanding in the wear mechanisms and in their changes, the compounds were abraded against abrasive papers of very different main asperities (grit size). This study covered also the assessment of the mechanical, fracture mechanical and viscoelastic behaviors of the rubbers.

Experimental

Materials

The composition of the peroxide curable HNBR was the following: HNBR (Therban® 3407 of Lanxess, Leverkusen, Germany; acrylonitrile content: 34 ± 1 %, residual double bonds: ≤ 0.9%, Mooney viscosity ML(1+4)100°=70 ± 7) – 100 part; zinc-containing mercapto-benzimidazole compound (Vulcanox® ZMB 2/C5 of Lanxess) - 0.5 part, t-butylperoxy-diisopropyl benzene (Perkadox 14-40 of Akzo-Nobel, Düren, Germany; active peroxide content: 40%) - 7 part, MgO -2 part, triallyl isocyanurate (TAIC 70 of Kettlitz-Chemie, Rennertshofen, Germany; active compound: 70%)-2.1 part and diphenylamine-based thermostabilizer (Luvomaxx CDPA of Lehmann & Voss, Hamburg, Germany) – 1.5 part. In this mix 35 part per hundred rubber (phr) carbon black (CB – high abrasive furnace, type N330, BET surface area: 70-99 m^2/g) or silica (Vulkasil A1 of Lanxess; precipitated sodium aluminum silicate with a medium reinforcing effect, BET surface area: 50 - 80 m^2/g). Silica, abbreviated further by SI, was also *in situ* silanized (SI-si) by vinyltrimethoxysilane (Evonik Industries, Essen, Germany) added in the recipe at 2 phr during compounding. The above recipe formulations were crosslinked at T=180 ^oC for 12 min into sheets of about 2 mm thickness. Specimens for the investigations listed below were cut/punched from these sheets.

Testing

Dynamic-mechanical thermal analysis (DMTA)

DMTA spectra were recorded on rectangular specimens (length x width x thickness = 20 x 10 x ca. 2 mm^3) in tension mode as a function of temperature (from -100 °C to

+100 °C) and a frequency of 10 Hz using a Q800 device of TA Instruments (New Castle, DE, USA). Tests were run at a constant strain (0.1%) with a heating rate of 2 ^{o}C/min. DMTA served also to determine the Payne effect caused by the fillers. It was investigated also in tensile mode, however, at 30°C using 10 Hz frequency with a strain sweep from 0.01 to 10% strain (denoted as M0.01 and M10, respectively).

Mechanical properties

The Shore A hardness of the rubbers, determined according to ISO 868 using a hardness measuring device of Zwick (Ulm, Germany) were: HNBR-CB:63^{o}, HNBR-SI:62^{o} and HNBR-SI-si:63^{o}. This was in line with our aim to produce and test formulations of identical hardness. Recall that this was achieved by selecting reinforcing fillers of similar BET surface areas.

Tensile tests were carried out dumbbells (type: S1 according to DIN 53504) on a Zwick Z250 (Ulm, Germany) universal testing machine at a deformation rate of 500 mm/min. From the related stress-strain curves apart from the ultimate properties, the stress values at 100, 200 and 300% elongations, termed M-100, M-200 and M300, respectively, were also read (ISO 37). To determine the tear strength at 500 mm/min deformation rate the recommendation of the ISO 34-1 standard (angle-type specimen with cut) was followed. To assess the Mullins effect (strain softening) the same specimen was subjected to loading (to 50, 100, 150 ad 200%, respectively)/complete unloading cycles successively. Each of above tests was done on five parallel specimens.

Fracture mechanical tests

Fracture mechanical tests were performed on single edge-notched tensile loaded (SEN-T) and trouser tear specimens. SEN-T specimens of 100 x 25 x 2 mm dimension (length x width x thickness) with 10 mm initial notch length were loaded with 10 mm/min crosshead speed on the above mentioned universal testing machine. The crack tip opening displacement (CTOD) has been followed by visual inspection using a CCD camera. The camera was positioned in front of the crack in order to focus on the internal surfaces of the blunting and growing crack. The crack surfaces were coated by talc for contrasting purpose. By analyzing the videotaped sequence the point where fracture started to propagate could be detected, and the corresponding J-integral value determined. J-integral tests were also performed on

specimens which were loaded up to 100% deformation at 200 mm/min crosshead speed in five cycles in order to eliminate the Mullins effect. Further details to this test can be taken from refs. [10-11]. The fracture energy from trouser tear ($J_{trouser}$) was determined on 100 x 30 x 2 mm specimens (length x width x thickness) with an initial notch length of 40 mm at 100 mm/min deformation rate. Like the mechanical, also the fracture mechanical tests were run on five parallel specimens.

Abrasive tests

The abrasion behavior of the samples was investigated by means of a custom-built scratch machine (Surface Machine Systems, College Station, TX, USA). A cylindrical flat rubber specimen with diameter of 5 mm was pressed and moved in the y-direction against an abrasive SiC-paper (Matador waterproof) thereby measuring the friction force continuously with a suitable load cell. The normal load was set to 8.4 N which is equivalent to a nominal pressure of 0.43 MPa, and the velocity was 5 mm/s. The sample was tested in a single pass mode, i.e. it was always in contact with the virgin surface of the abrasive paper (Figure 1). The grit size of the abrasive papers was varied using P600 (grit size: 25.8±1 µm), P1200 (grit size: 15.3±1 µm), P2500 (grit size: 8.4±0.5µm), P3000 (grit size: 7µm), and P5000 (grit size: 5µm) types, respectively. All tests were run at room temperature. The coefficient of friction (COF) was measured online and after the tests the specific wear rate was calculated according to Equation 1:

$$W_s = \frac{\Delta m}{\rho \cdot F \cdot L} \qquad (1)$$

where Δm is the mass loss of the specimen measured gravimetrically, ρ is the density, determined by the buoyancy method in water, *F* is the normal force (i.e. 8.4 N) and *L* is the overall sliding distance (0.5 m).

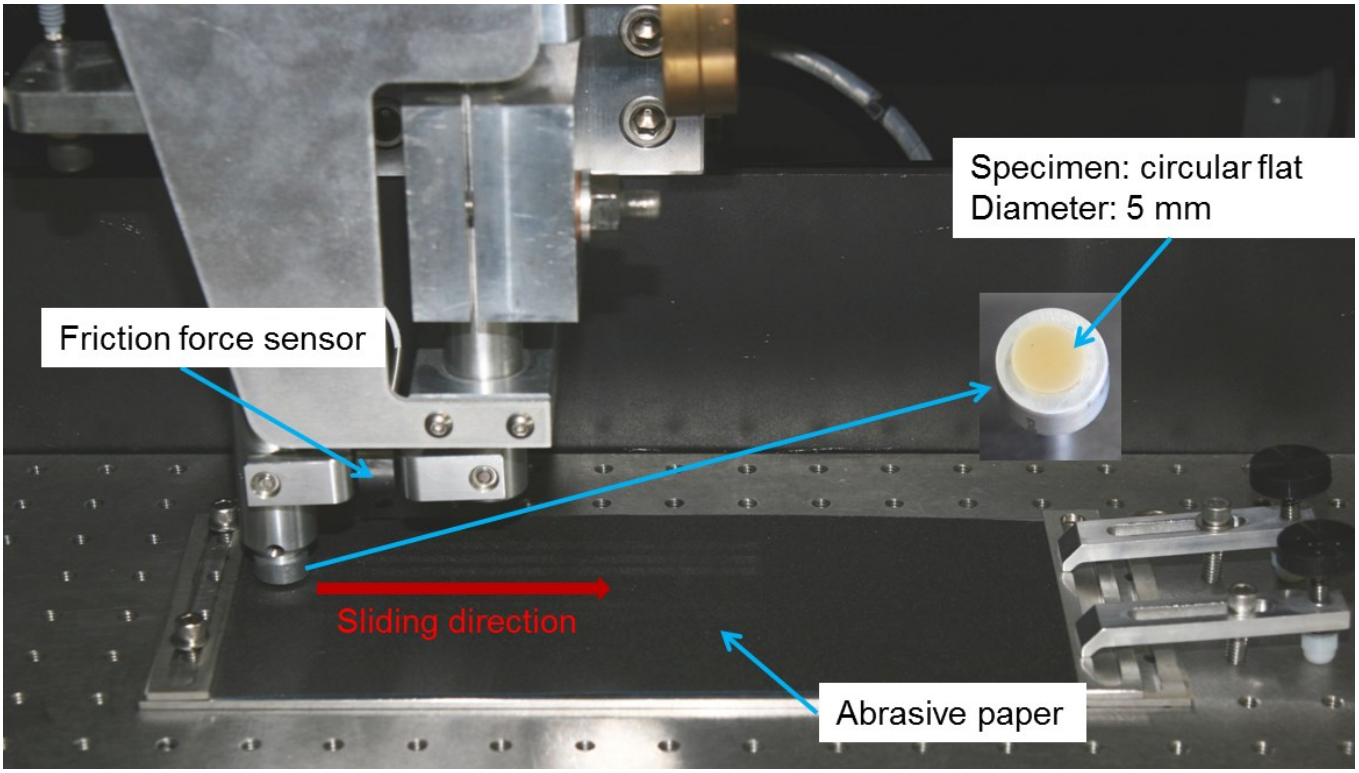

Figure 1: Rig for abrasion testing

Wear mechanisms

The worn surfaces of the specimens were inspected by a scanning electron microscope (Supra 40 Zeiss, Oberkochen, Germany). Prior to SEM investigations the specimens were sputtered with ultra-thin layer of Au/Pd alloy.

Results and Discussion

HNBR characteristics

Based on the storage modulus vs. temperature (E' vs T) traces there is no difference between the HNBR rubbers in the glassy state. In the rubber state the HNBR-CB and HNBR-SI show similar plateau values by contrast to HNBR-SI-si lying below them (Figure 2a). Judging about the reinforcing actions of the fillers considering the decrease of the mechanical loss peak (tan δ) the ranking is: CB>SI>SI-si (cf. Figure 2b). The glass transition temperature (T_g) was not influenced by the type of the fillers used irrespective whether the loss modulus (not given here) or the tan δ vs. T traces (Figure 2b) were considered. According to the rubber elasticity theory the inverse of the plateau modulus ($1/E_{pl}$) at a given temperature above T_g correlates with the mean molecular mass between crosslinks (M_c):

$$M_c = \frac{3.\rho.RT}{E_{pl}} \qquad (2)$$

where E_{pl} is the modulus at T= 296 K, ρ is the density, R is the universal gas constant (8.314 J/(K.mol), and T is the absolute temperature (i.e. T=296 K). It has to be underlined that M_c is an apparent value because it implies not only the crosslinking but also the rubber-filler and filler-filler interactions. The M_c data for HNBR-CB, -Si and SI-si were 676, 771 and 1014 g/mol, respectively.

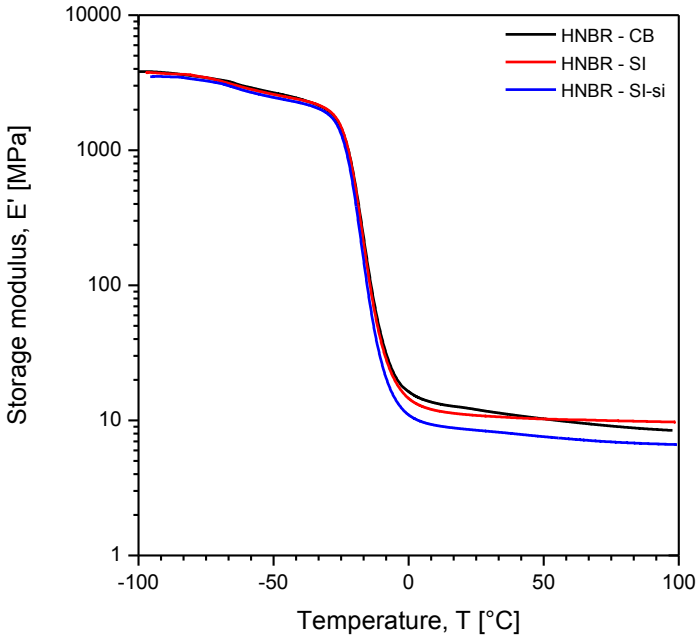

a)

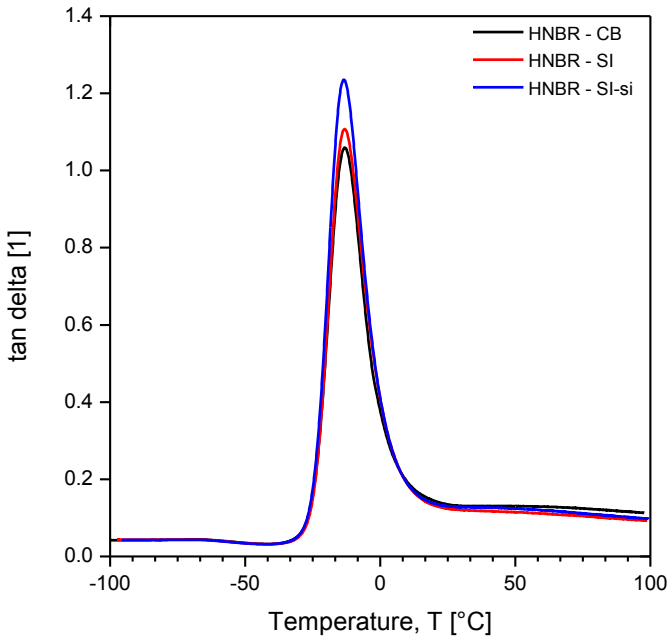

b)

Figure 2: a) Storage modulus (E') vs temperature (T) and b) mechanical loss factor (tanδ) vs T traces for the HNBR rubbers studied

The Payne effect was the most and least pronounced for CB and Si-si nanofillers, as expected (cf. Figure 3). It was quantified by the difference M0.01-M10.

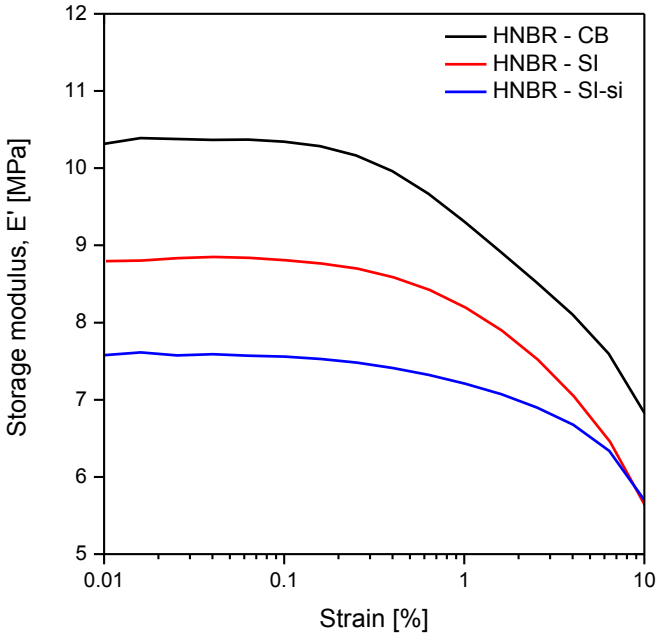

Figure 3: E' vs. tensile strain traces for the HNBR rubbers measured at T=30 ^{o}C

Mechanical tests

The tensile tests results are tabulated in Table 1. Different tendencies can be observed for strength- and ductility-related parameters as a function of the fillers' type. Nonetheless, CB outperformed the silica fillers with respect to tensile strength data. Silane treatment of the silica enhanced prominently the moduli at different strains compared to the untreated one but did not affect the ultimate tensile strength. Silane treatment was associated with a reduction in the ultimate tensile strain (cf. Figure 4 and Table 1). Interestingly, the highest tear strength exhibited HBNR-SI followed by HNBR-CB and HNBR-SI-si.

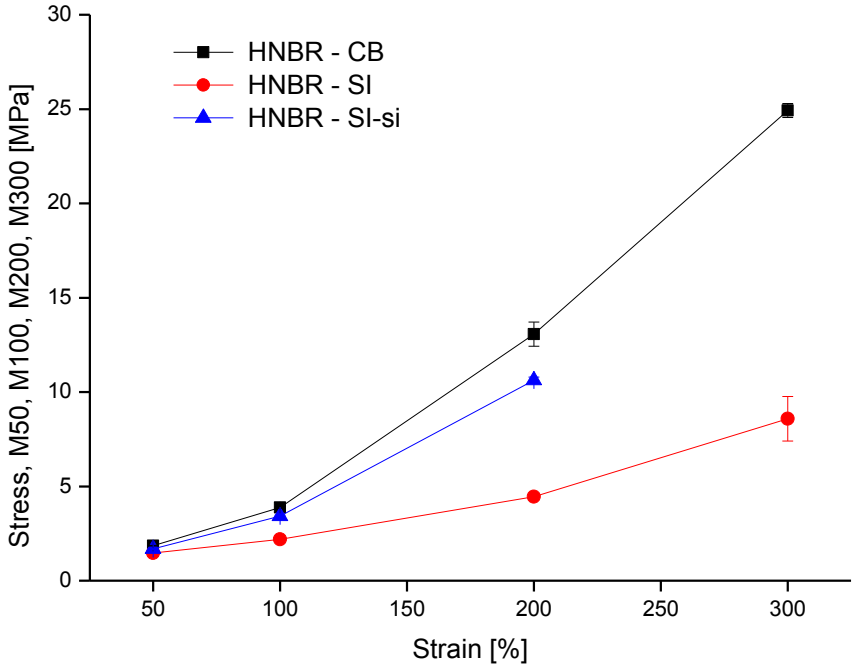

Figure 4: Moduli at different strain values for the HNBRs tested

Figure 5 informs us about the Mullins effect in the rubbers. In this Figure the first and fifth cycles of stress-strain curves up to 150% of the compounds which were previous loaded up to 100% strain are depicted. For comparison purpose the stress-strain curves of the rubbers at the first monotonic loading are also indicated. The Mullins effect has been quantified by considering the force ratio of the cyclic (F_1..F_5) and separate monotonic loading (F_0) of the specimens at a given strain as a function of the loading cycles (1 to 5). Change in the dissipated energy (E_{diss}) has been considered in a similar way as that of the force (cf. Figure 5). The corresponding data are also listed in Table 1.

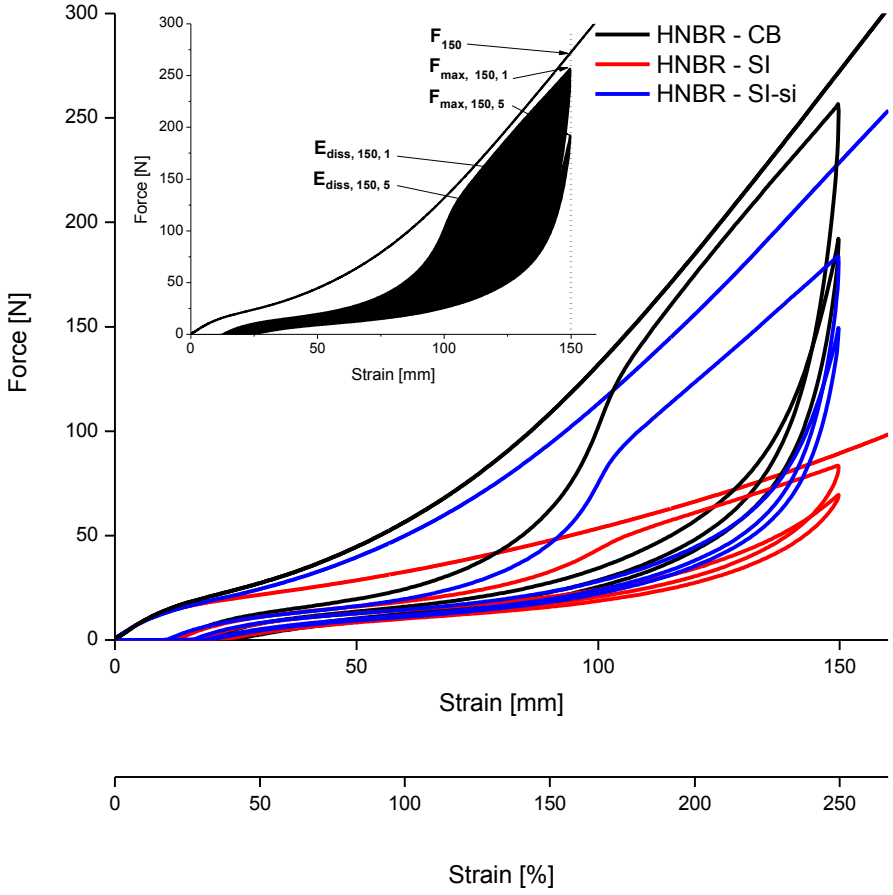

Figure 5: Mullins effect in the first and fifth cycles of loading up to 150 mm strain of the HNBR specimens subjected previously to five cycles up to each 50 and 100 mm strains, respectively

Fracture mechanical results

The J-integral vs. CTOD traces of the specimens with and without cyclic preloading are summarized in Figure 6. These traces could well be approximated by the function:

$$J = a - b \cdot c^{CTOD} \qquad (3)$$

where a, b and c are fitting constants and the value of c is always below 1. Equation 3 can be reasoned by the fact that the value of “a” agreed reasonably with the measured J-integral upon full specimen separation (J_{total}).

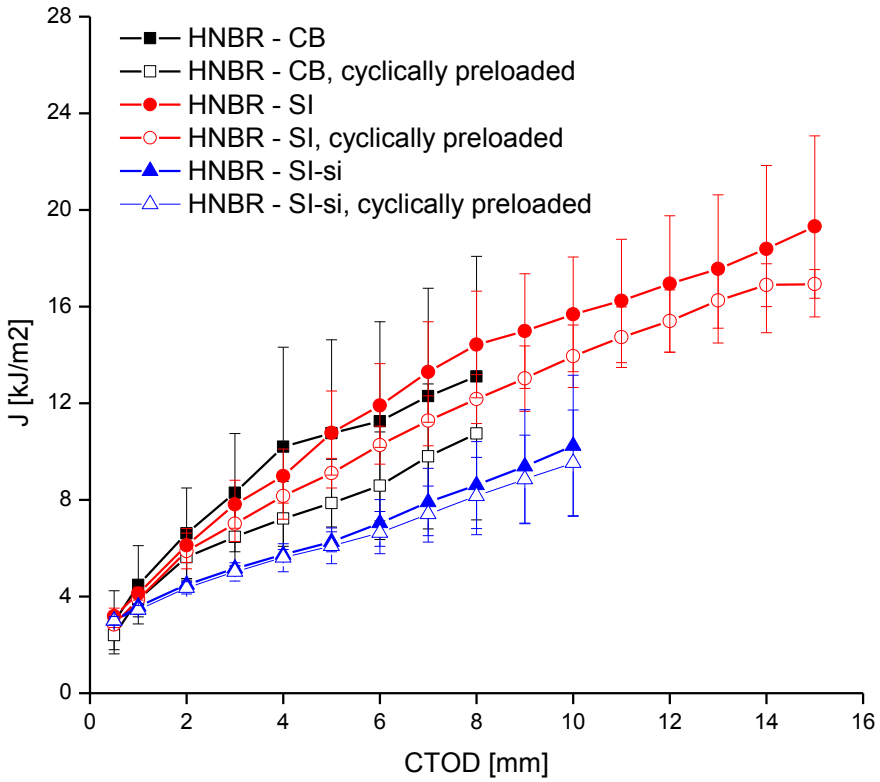

Figure 6: J vs. CTOD traces for the HNBR specimens with and without cyclic preloading

Results in Figure 6 indicate that cyclic preloading resulted in slightly lower J-integral values in the related resistance curves. The critical value of the J-integral, assigned to the onset of crack growth, has been read at CTOD=0.5 mm. This was recommended by the group of Riccò [10,11]. Figure 7 shows that practically identical J_c values have been found for the HNBR rubbers tested. Cyclic preloading slightly reduced the J_c data suggesting some effect of Mullins strain softening. The only exception was SI-si filler for which the lowest Mullins and Payne effects were found. The largest scatter in J_c was noticed for HNBR-CB reflecting the most pronounced filler-filler interactions between the CB particles in this mix.

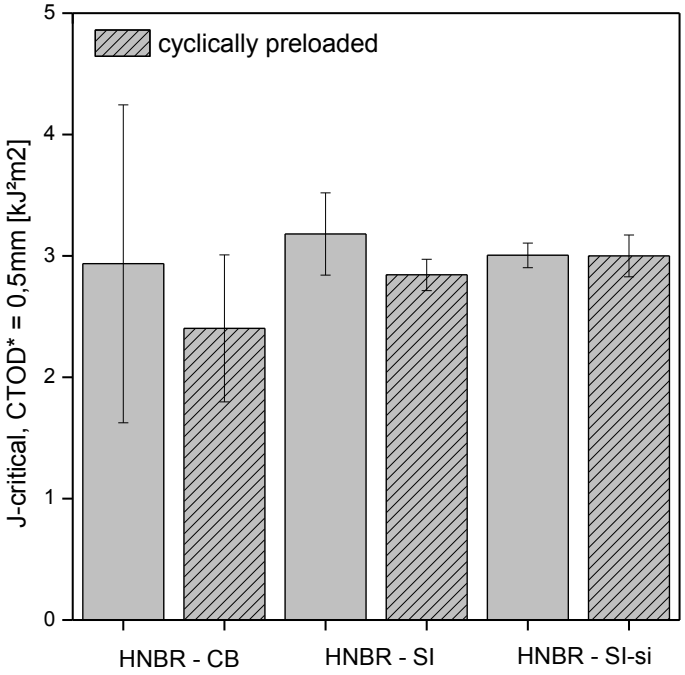

Figure 7: Comparison of the J_c data for the HNBR specimens with and without cyclic preloading

$J_{trouser}$ was determined by the following Equation [12]:

$$J_{trouser} = \frac{2 \cdot F_{tear}}{t} \qquad (4)$$

where F_{tear} is the mean force during stable tearing and t is the specimen thickness. Values of $J_{trouser}$ are in between J_c and J_{total}, closer to the latter, as expected based on the fact that it represents a steady crack growth. In order to complete the toughness determination the absorbed energy during monotonic tensile loading was also calculated. For that purpose the surface below the strength vs. deformation curve was integrated.

Abrasive friction and wear

Figure 8 summarizes the effects of filler types and grit size of the abrasive paper on the COF. One can recognize that the COF does not depend on the type (grit size) of the abrasive paper. On the other hand, the fillers do influence the COF. The COF was decreasing according to the range: CB>SI-si>SI. Unexpectedly, the COFs of

HNBR-SI was slightly below those of HNBR-CB and HNBR-SI-si, the reason of which is not known by the authors. It is usually accepted that the COF may depend on the hardness of the polymer [13]. This is, however, not the case in this work because attention was paid to use HNBR gums of the same hardness (cf. Table 1).

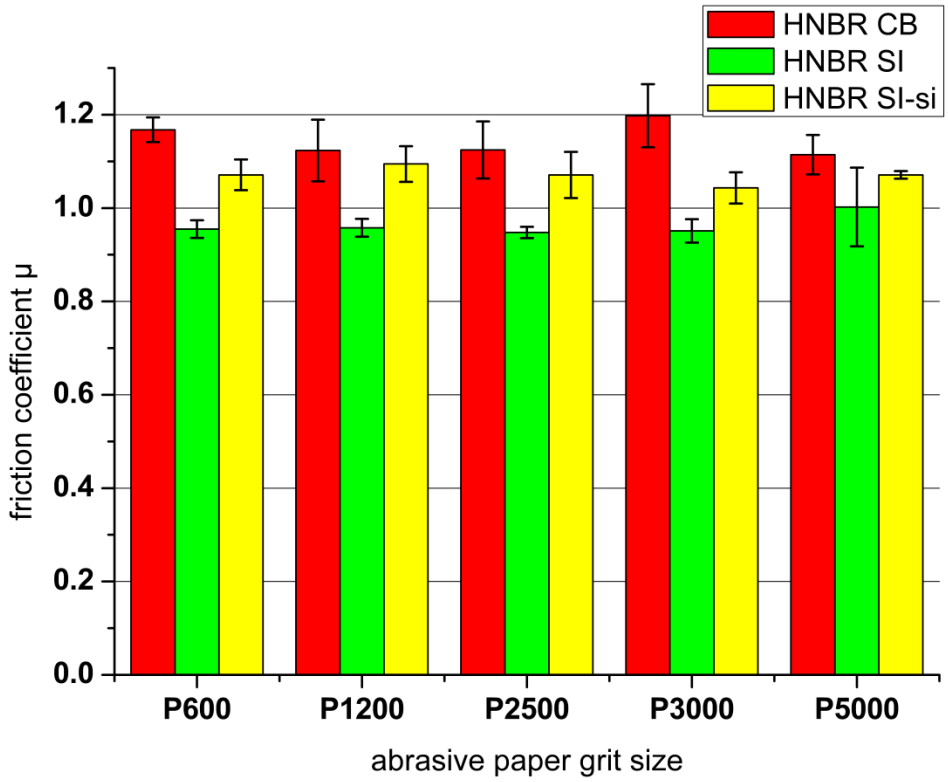

Figure 8: Comparison of the COF values for the HNBRs worn against abrasive papers of different grit sizes (Note: the grit size and thus the surface roughness of the abrasive papers decreases with increasing P numbers – see “Abrasive test” section)

One may suppose that the specific wear rate of the rubbers follows a similar trend as COF, i.e. the lower the COF the lower the specific wear rate is. The results do not substantiate this prediction. The ranking when considering lowest abrasion loss (i.e. highest resistance to abrasion) against all the abrasive surfaces is: CB > SI-si > SI (Figure 9). As expected, the specific wear rate decreases with reduction of the surface roughness (grit size) of the abrasive paper. The specific wear rate of the HNBR compounds did not change when the grit size of the abrasive papers was reduced from 7 to 5 μm. This was a common feature for all HNBR compounds tested (Figure 9). Considering the fact that the surface roughness of the counterpart under dry sliding conditions is at about 1 μm [3-6], the observed change can be assigned to a transition from abrasive toward sliding wear.

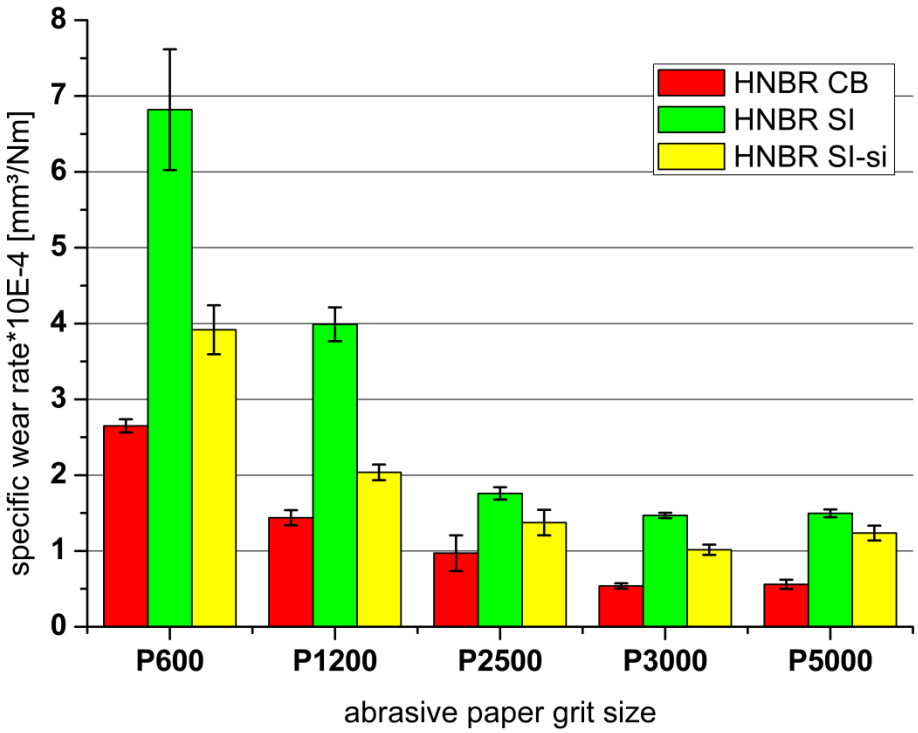

Figure 9: Comparison of the specific wear rates for the HNBRs worn against abrasive papers of different grit sizes. For note cf. Figure 9.

Wear mechanisms

The worn tracks of the HNBR compounds were inspected in SEM (cf. Figures 10-12). Figure 10 compares the surfaces of the HNBRs worn against the coarsest abrasive paper. One can clearly see the grooves, scratches on the worn surfaces caused by the grits. On the other hand, no ridges, lying perpendicular to the abrasion direction could be detected. The latter was often observed during abrasion wear [14-15]. Note that in the first approximation the roughness of the worn surface inversely correlates with the wear resistance of the materials. Accordingly, based on the apparent roughness of the worn surfaces in Figure 10 the following ranking can be deduced for the specific wear rate: HNBR-CB < HNBR-SI-si < HNBR-SI. This is in full agreement with the results (cf. W_s data against P600 in Figure 9).

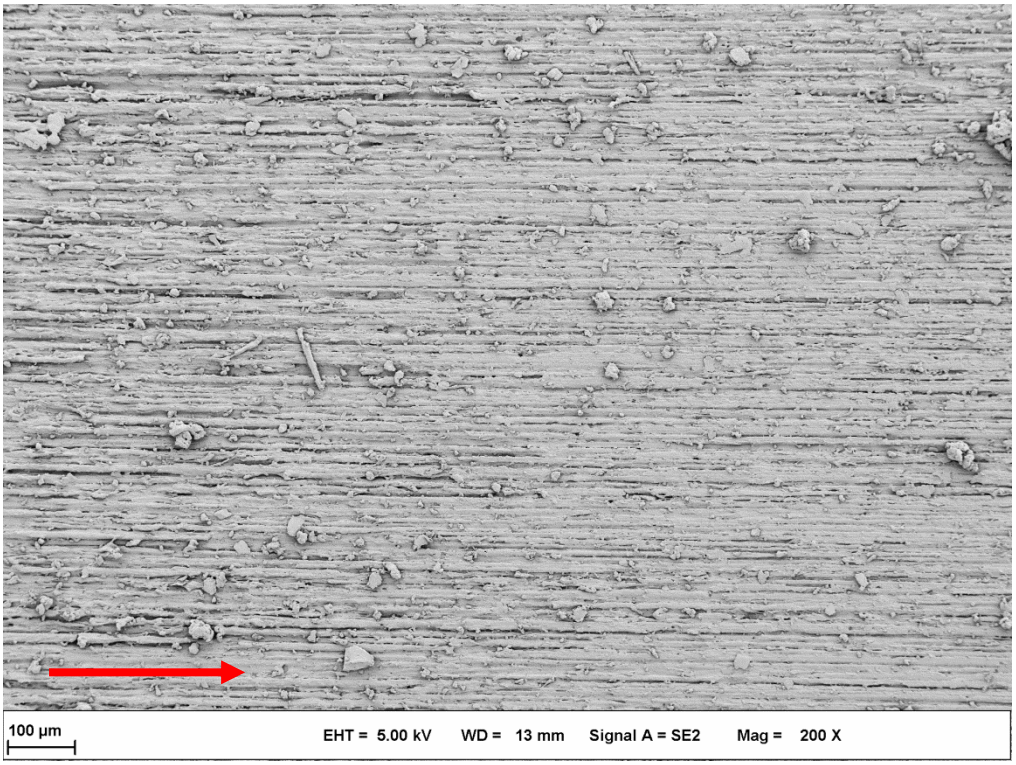

(a) HNBR-CB

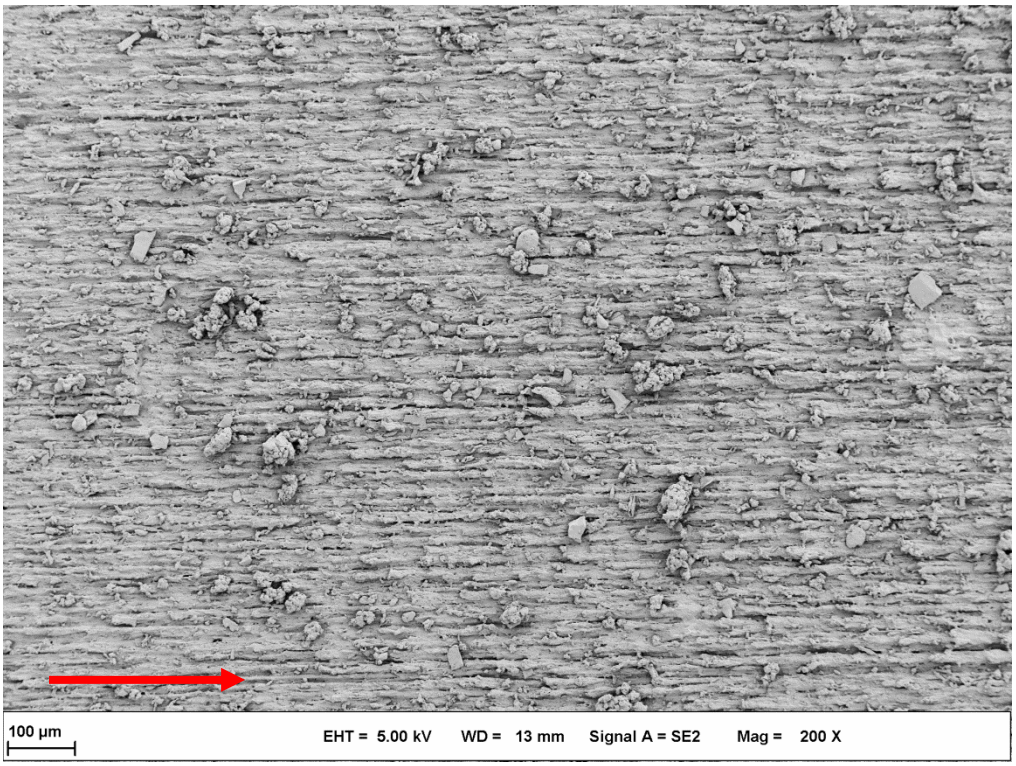

(b) HNBR-SI

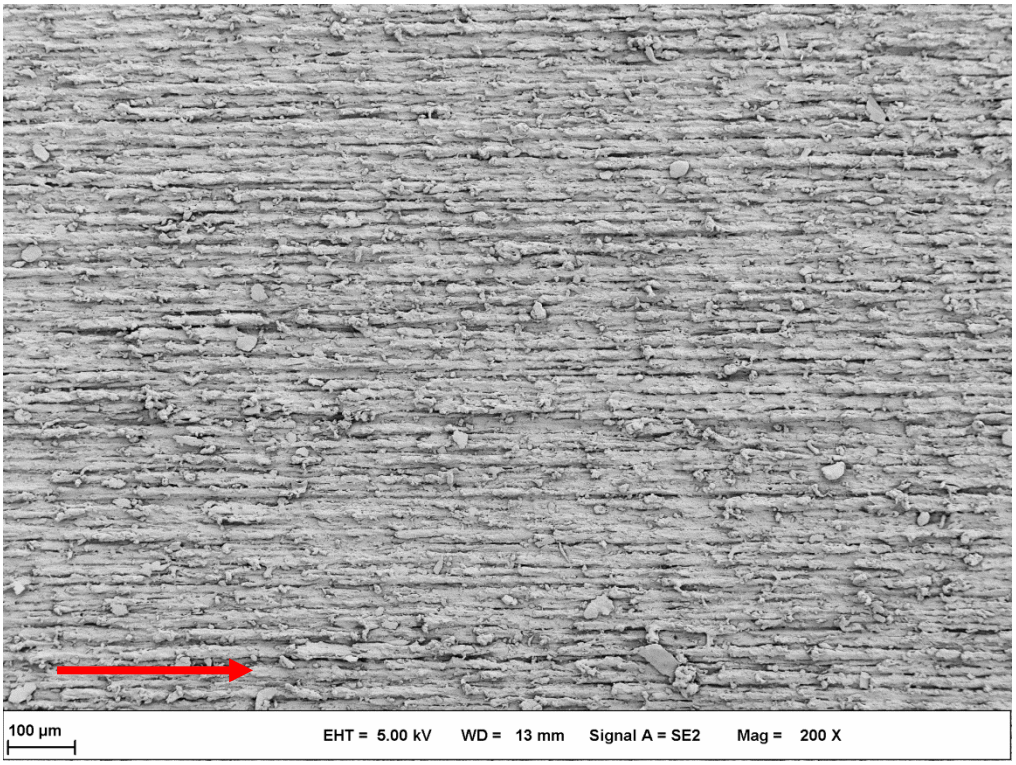

(c) HNBR-SI-si

Figure 10: SEM pictures taken from the wear tracks after the abrasive tests (a) HNBR-CB, (b) HNBR-SI, and (c) HNBR-SI-si against P600 abrasive paper. Note: arrow indicates the sliding direction

Comparing the worn tracks of HNBRs with the best and poorest abrasion resistances further insight in the wear mechanisms can be revealed (Figure 11).The debris are obviously formed by ploughing and chipping when the rubbers were worn against P600 paper.

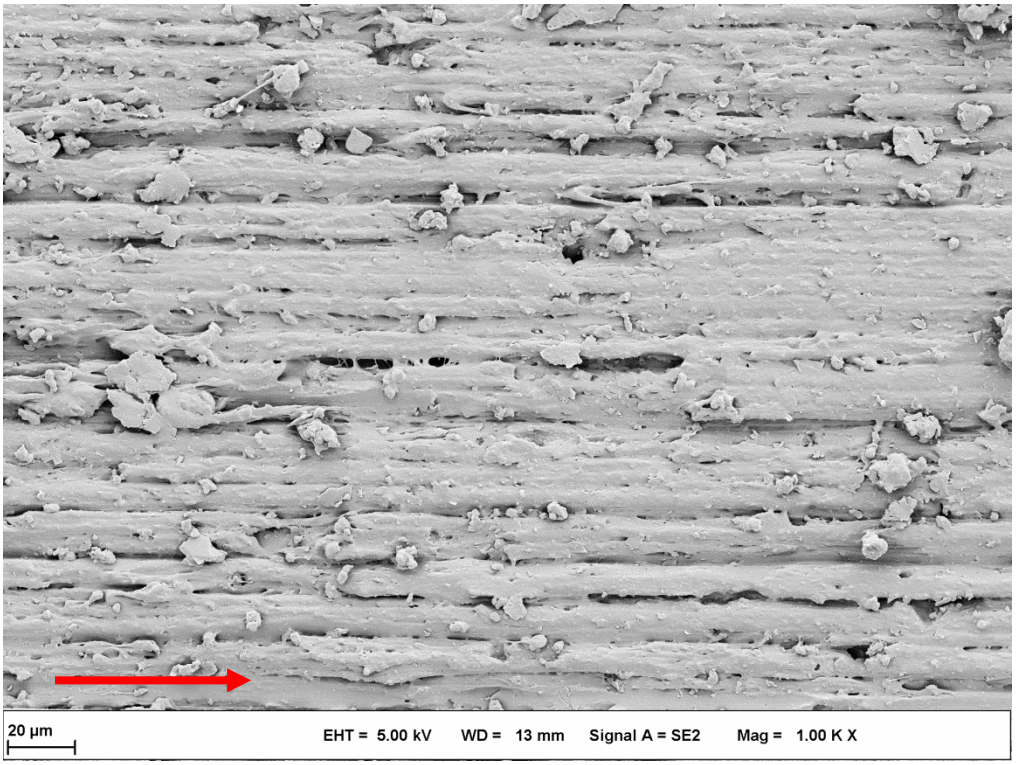

(a) HNBR-CB

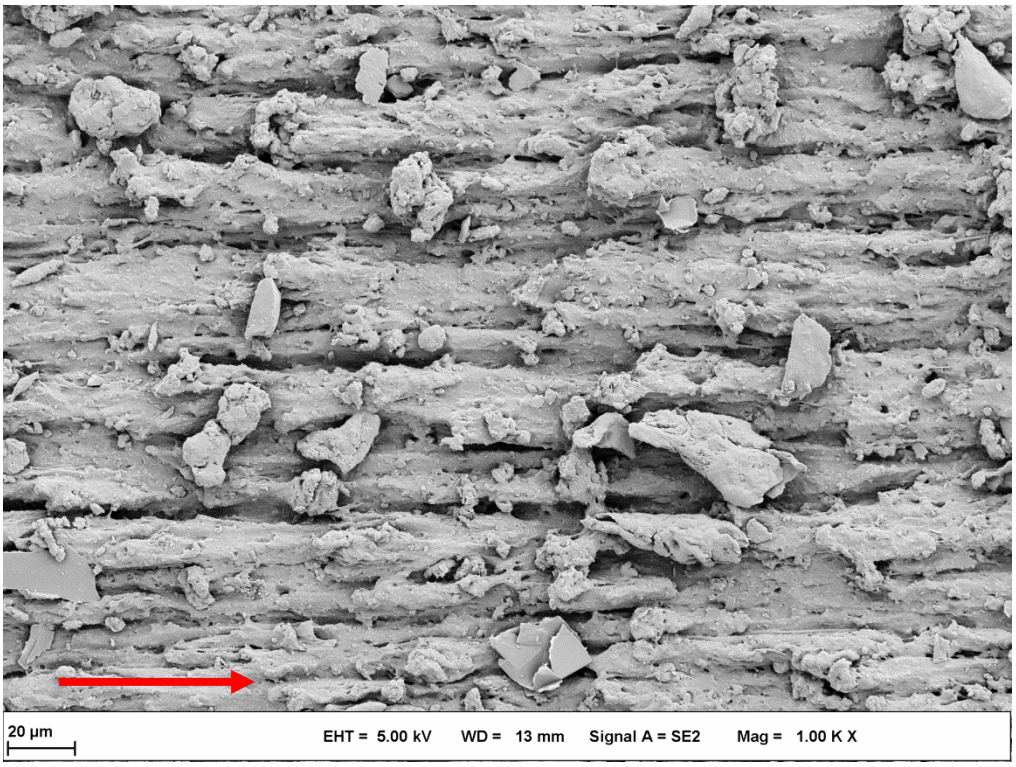

(b) HNBR-SI

Figure 11: SEM pictures taken from the wear tracks after the abrasive tests against P600 type abrasive paper. Designations: (a) HNBR-CB and (b) HNBR-SI. Note: sliding direction is indicated by arrow

Recall that with decreasing grit size the abrasive wear is highly reduced (cf. Figure 9). In order to show the changes in the wear mechanisms the worn surfaces of HNBR-CB and HNBR-SI, respectively, are compared after abrasion against P2500 type paper in Figure 12.

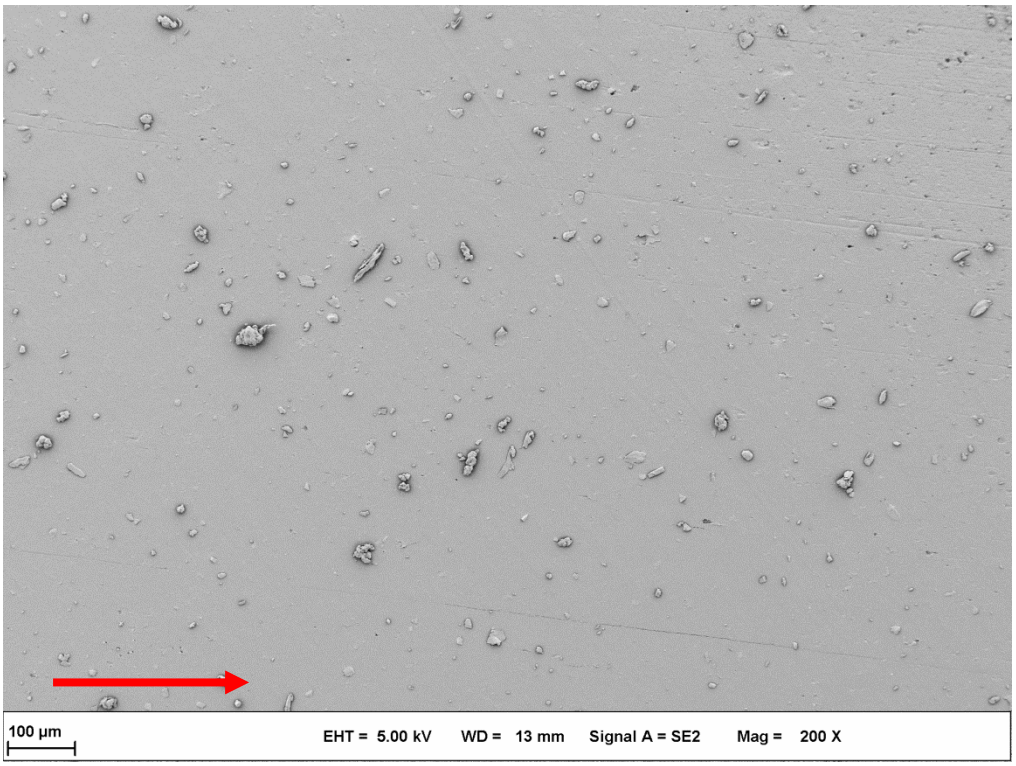

(a) HNBR-CB

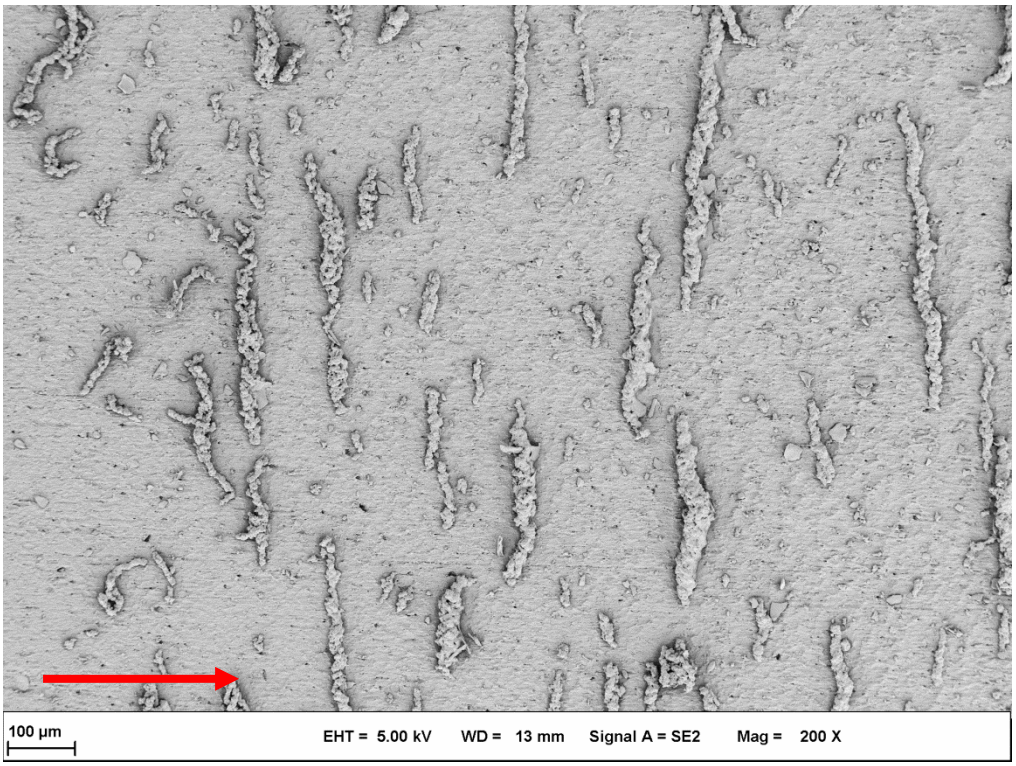

(b) HNBR-SI

Figure 12: SEM pictures taken from the surfaces abraded against P2500 type abrasive paper. Designations: (a) HNBR-CB and (b) HNBR-SI. Note: sliding direction is indicate by arrow

By contrast to HNBR-CB showing small particulates, rolled debris appear on the abraded surface of HNBR-SI. The latter are oriented transverse to the abrasion direction. On the other hand, no clear Schallamach-type wavy pattern, which is often observed during dry sliding wear of rubbers [16], is present in Figure 12b.

Abrasion against the finest abrasive paper (P5000) resulted in the lowest specific wear rates measured. HNBR-CB performed better than the silica filled versions under this abrasion condition, too. On the other hand, the specific wear rates of HNBR-SI and HNBR-SI-si were practically the same (cf. Figure 10). This suggests that the same wear mechanisms were at work. In fact, this is well documented by SEM pictures taken from the abraded surfaces in Figure 13.

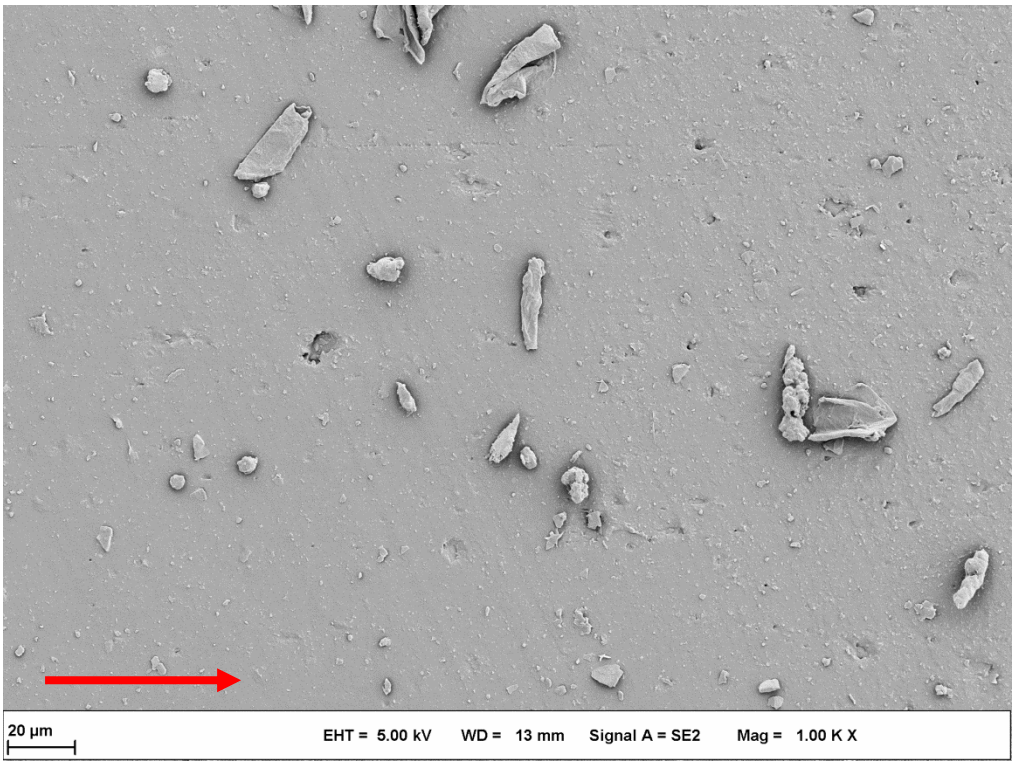

(a) HNBR-CB

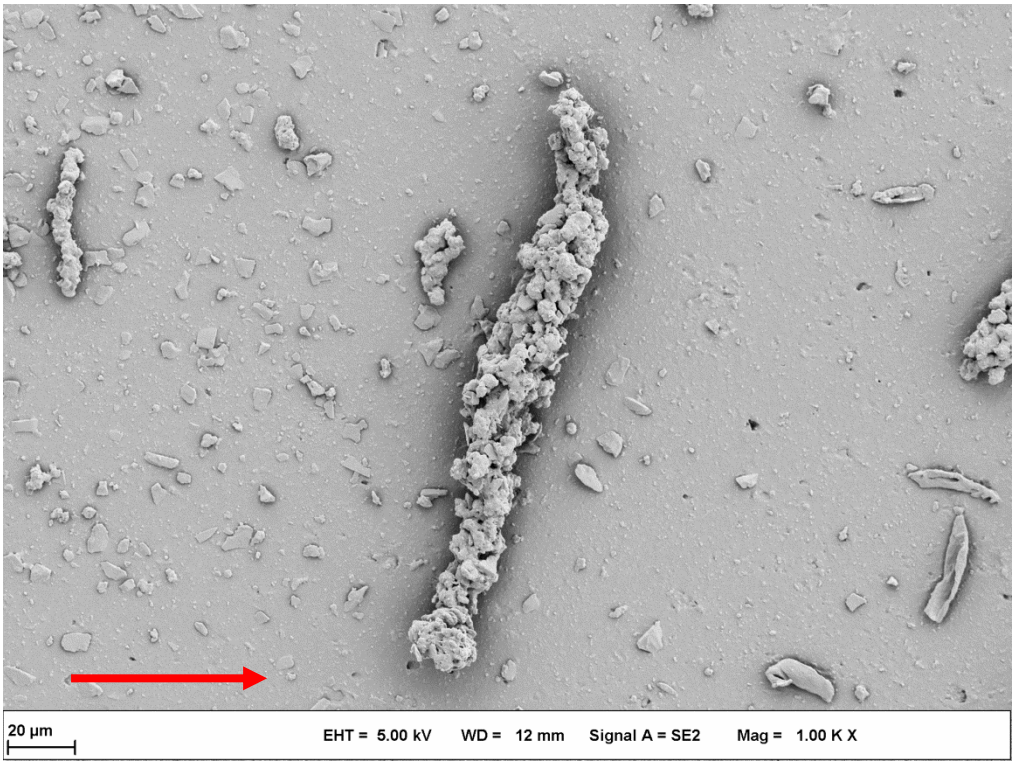

(b) HNBR-SI

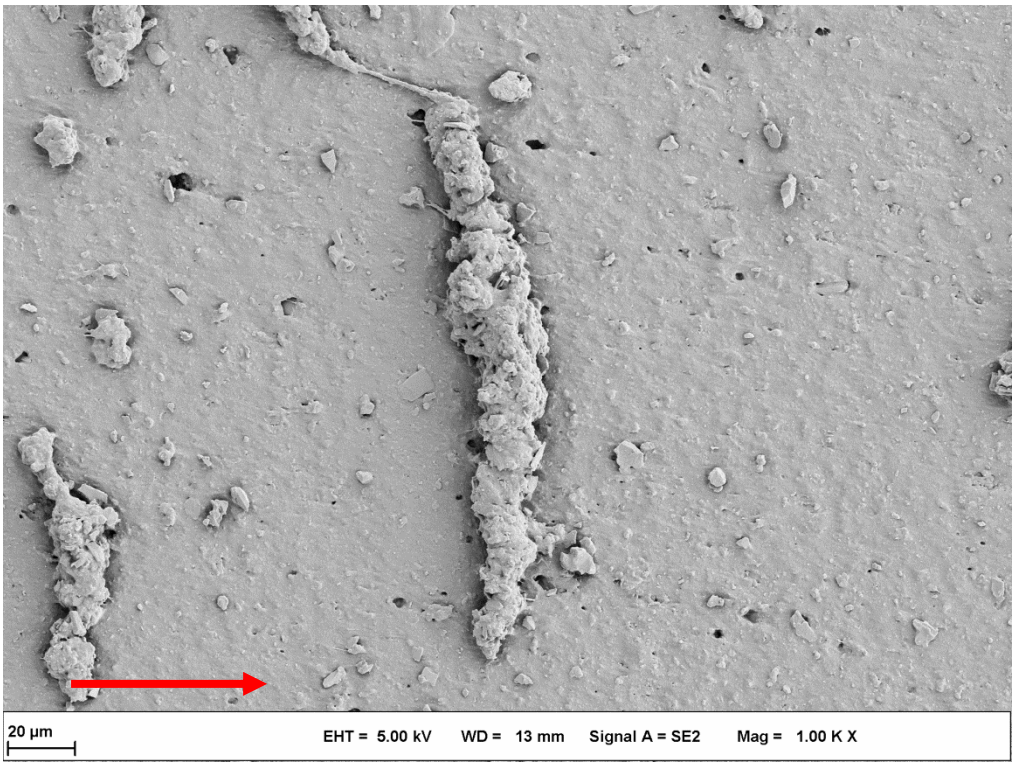

(c) HNBR-SI-si

Figure 13: SEM pictures taken from the surfaces of the rubbers abraded against P5000 abrasive paper. Designations: (a) HNBR-CB, (b) HNBR-SI, and (c) HNBR-SI-si. Note: sliding direction is indicated by arrow

The particulate debris in HNBR-CB were formed by pitting. This mechanism was even more effective in the silicate-filled gums. The pitted particles on the worn surfaces of HNBR-SI and HNBR-SI-si agglomerated in microrolls. These microrolls were more “rubberized” for HNBR-SI-si than for HNBR-SI (cf. Figure 13b and c). This hints that the silane compound introduced acted for the filler/matrix adhesion properly.

Possible correlations with wear rate

According to the above wear mechanisms, discussed in connection with Figures 10-13, one gets the impression that there should be some correlation between the wear resistance and some structure-, viscoelasticity-related or (fracture) mechanical properties. As the wear mechanisms alter as a function of the abrasive counterface (cf. Figures 11 and 13) the correlating properties, if any, may also change. The SEM results suggest that toughness-related parameter may govern the wear rate for highly abrasive, while viscoelasticity-related ones the wear at less abrasive (i.e. sliding-type) conditions. Nevertheless, the resistance to abrasive wear of the studied compounds follows the ranking: HNBR-CB > HNBR-SI-si > HNBR-SI (cf. Figure 9). Constructing a correlation matrix in which all the measured properties are listed and ranked, however, we do not get any clear correlation between the wear resistance and measured properties. This may be linked with one or more of the following arguments. First, wear is a system property, as often quoted and thus correlation with material properties is *per se* excluded. Second, possible correlation may exist when wear is treated as a function of combined terms of rubber-related properties. This was, however, beyond the scope of this contribution. Third, the rubbers involved, though carefully chosen, show similar wear performance. Note that the specific wear rates changed by a factor of 2 which is much too low in usual tribological tests to deduce reliable correlations. Forth, the number of rubber compounds in this work was too low and far more of them have to be tested in order to generate a suitable database. Nonetheless, the authors are convinced that eventual correlation with the wear performance can only be deduced when considering the properties, including their change as a function of frequency and temperature, studied.

Conclusion

This study was devoted to investigate the mechanical and abrasive wear properties of a peroxide cured HNBRs having the same Shore A hardness (62-63°) set by incorporating different fillers, viz. carbon black (CB), silica (SI) and silanized SI (SI-si). The rubbers were worn against abrasive papers of different grit sizes (P600-P5000). Attempt was made to find correlation between the mechanical and abrasive wear properties. Based on this work the following conclusions can be drawn:

1. The fillers selected yielded compounds with identical Shore hardness. Based on the DMTA response CB provided the best reinforcement followed by SI and SI-si. This ranking did not hold for the tensile and tear strength data. *In sit*u silanization enhanced the moduli at different strains, reduced the ultimate elongation but not affected the ultimate tensile strength. Silanization was helpful to reduce the Payne- and Mullins-effects, as well. The critical J-integral, linked with crack initiation, was practically the same for the HNBRs. The J-values deduced from trouser tear and full separation of the SEN-T specimens were closer to one another and followed the same tendency, i.e. HNBR-SI-si < HNBR-CB < HNBR-SI. Cyclic preloading of the related specimens, to avoid the Mullins-effect, yielded somewhat lower J-data.
2. Values of the coefficient of friction (COF) did not depend on the grit size of the abrasive paper. On the other hand, its value depended on the filler type. The specific wear rate was markedly lowered with reduced grit size of the abrasive paper. The specific wear rate was not further reduced when the mean grit size changed from 7 μm (P3000) to 5 μm (P5000). The wear mechanism changed with decreasing grit size from ploughing, tearing, chipping to pitting associated with roll formation.
3. Between the determined properties and the wear resistance of the investigated HNBRs (viz. HNBR-CB > HNBR-SI-si > HNBR-SI) no definite correlation could be traced. Possible reasons behind this finding were summarized.

Acknowledgement

The HNBR samples were provided by Lanxess (Leverkusen, Germany that is gratefully acknowledged.

References

1 B. J. Briscoe, S. K. Sinha: Tribological applications of polymers and their composites. Past, present and future prospects in “Tribology of Polymeric Nanocomposites” (Eds.: K. Friedrich, A. K. Schlarb), Elsevier. Amsterdam, 2008, Ch.1, pp. 1-14

2 C. Wrana, K. Reinartz, H. R. Winkelbach: Therban® - The high performance elastomer for the new millennium, Macromol. Mater. Eng. 286 (11) (2001) 657-662.

3 D. Felhös, J. Karger-Kocsis, D. Xu: Tribological testing of peroxide cured HNBR with different MWCNT and silica contents under dry sliding and rolling conditions against steel, J. Appl. Polym. Sci. 108 (2008) 2840-2851.

4 D. Xu, J. Karger-Kocsis: Rolling and sliding wear properties of hybrid systems composed of uncured/cured HNBR and partly polymerized cyclic butylene terephthalate (CBT), Tribol. Intern. 43 (2010) 289-298.

5 J. Karger-Kocsis, D. Felhös, D. Xu: Mechanical and tribological properties of rubber blends composed of HNBR and in situ produced polyurethane, Wear 268 (2010) 464-472.

6 D. Xu, J. Karger-Kocsis, A. K. Schlarb: Friction and wearof HNBR with different fillers under dry rolling and sliding conditions, Express Polym. Lett. 3(2) (2009) 126-136.

7 P. Thavamani, A. K. Bhowmick: Influence of compositional variables and testing temperature on the wear of hydrogenated nitrile rubber, J. Mater. Sci. 28 (1993) 1351-1359.

8 Z. Wei, Y. Lu, Y. Meng, L. Zhang: Study on wear, cutting and chipping behaviors of hydrogenated nitrile butadiene rubber reinforced by carbon black and in situ prepared zinc dimethacrylate, J. Appl. Polym. Sci., 124 (2012) 4564-4571.

9 W. Arayapranee: Rubber abrasion resistance in “Abrasion Resistance of Materials”, (Ed.: M. Adamiak), InTech, Rijeka, 2012, Ch.8, 147-166.

10 S. Agnelli, G. Ramorino, S. Passera, J. Karger-Kocsis, T. Riccò: Fracture resistance of rubbers with MWCNT, organoclay, silica and carbon black fillers as assessed by the J-integral: Effects of rubber type and filler concentration, Express Polym. Lett. 6(7) (2012) 581-587.

11 G. Ramorino, S. Agnelli, R. De Santis, T. Riccò: Investigation of fracture resistance of natural rubber/clay nanocomposites by J-testing, Eng. Fract. Mech. 77 (2010) 1527–1536.

12 A. N. Gent, J. Jeong: Tear strength of oriented crystalline polymers, J. Mater. Sci. 21 (1986) 355-363.

13 G. Kalácska: An engineering approach to dry friction behaviour of numerous engineering plastics with respect to the mechanical properties, Express Polym. Lett. 7(2) (2013) 199-210.

14 P. Thavamani, D. Khastgir, A. K. Bhowmick: Microscopic studies on the mechanisms of wear of NR, SBR and HNBR vulcanizates under different conditions, J. Mater. Sci. 28 (1993) 6318-6322.

15 P. Junkong, P. Kueseng, S. Wirasate, C. Huynh, N. Rattanasom: Cut growth and abrasion behaviour, and morphology of natural rubber filled with MWCNT and MWCNT/carbon black, Polym. Test. 41 (2015) 172-183.

16 J. Karger-Kocsis, A. Mousa, Z. Major, N. Békési: Dry friction and sliding wear of EPDM rubbers against steel as a function of carbon black content, Wear 264 (2008) 359-367.

Tables

Table 1

Property [unit]		HNBR-CB	HNBR-SI	HNBR-SI-si
Shore A [°]		63	62	63
Density [g/cm^3]		1.120	1.146	1.149
M_c [g/mol]		676	771	1014
tan δ at Tg [1]		1.06	1.11	1.24
Payne effect, M0.01-M10 [MPa]		3.49	3.19	1.89
M-50 [MPa]		1.9±0.0	1.5±0.0	1.7±0.0
M-100 [MPa]		3.9±0.0	2.2±0.0	3.4±0.1
M-200 [MPa]		13.1±0.6	4.5±0.0	10.6±0.2
M-300 [MPa]		24.9±0.4	8.6±1.2	-
Tensile strength [MPa]		28.9±2.4	18.6±0.8	18.4±1.6
Tensile strain [%]		335±24	467±11	277±17
Tear strength [kN/m]		16.5±0.9	18.1±1.4	11.3±1.6
Mullins-effect [%]	$F_{max, 50, 1}$	88±4	91±2	75±1
	$F_{max, 50, 5}$	79±4	84±2	69±1

	$F_{max,\ 150,\ 1}$	92±2	94±2	81±1
	$F_{max,\ 150,\ 5}$	69±1	78±1	66±1
	$E_{diss,\ 50,\ 1}$	26±3	29±2	21±0
	$E_{diss,\ 50,\ 5}$	13±0	13±1	10±0
	$E_{diss,\ 150,\ 1}$	42±1	32±1	37±1
	$E_{diss,\ 150,\ 5}$	8±0	13±3	5±2
$J_{critical,\ CTOD^*=0.5mm}$ [kJ/m^2]		2.94±0.61	3.18±0.34	3.00±0.10
$J_{critical,\ CTOD^*=0.5mm}$, cyclically preloaded [kJ/m^2]		2.40±0.61	2.84±0.13	2.99±0.17
J_{total} [kJ/m^2]		17.88±1.65	28.20±8.38	10.52±2.94
J_{total}, cyclically preloaded [kJ/m^2]		15.85±5.99	26.96±9.06	10.58±1.78
Absorbed energy in tensile test [kJ/m^2]		2719	2008	1396
$J_{trouser}$ [kJ/m^2]		9.05±0.91	14.34±1.81	7.59±0.58